ANNALS of Clinical and Translational Neurology
Open Access
ANA American Neurological Association since 1875

RESEARCH ARTICLE

Sulfatide levels correlate with severity of neuropathy in metachromatic leukodystrophy

Christine í Dali[1], Norman W. Barton[2], Mohamed H. Farah[3], Mihai Moldovan[4,5], Jan-Eric Månsson[6], Nitin Nair[2], Morten Dunø[1], Lotte Risom[1], Hongmei Cao[2], Luying Pan[2], Marcia Sellos-Moura[2], Andrea M. Corse[3] & Christian Krarup[4,5]

[1]Department of Clinical Genetics, Rigshospitalet, Copenhagen, Denmark
[2]Shire, Lexington, Massachusetts
[3]Department of Neurology, Johns Hopkins Medical Institutions, Baltimore, Maryland
[4]Department of Clinical Neurophysiology, Rigshospitalet, Copenhagen, Denmark
[5]Department of Neuroscience and Pharmacology, University of Copenhagen, Copenhagen, Denmark
[6]Clinical Neurochemistry Laboratory, Sahlgrenska University Hospital, Gothenburg, Sweden

Correspondence
Christian Krarup, Department of Clinical Neurophysiology, Rigshospitalet, Blegdamsvej 9, 2100 Copenhagen, Denmark. Tel: +45 3545 3060; Fax: +45 3545 3264; E-mail: Christian.krarup@regionh.dk

Funding Information
The study was sponsored by Shire. Support was provided by the Danish Medical Research Council, the Lundbeck Foundation and the Novo Nordisk Foundation (M. M., C. K.).

Received: 1 February 2015; Accepted: 4 February 2015

Annals of Clinical and Translational Neurology **2015; 2(5): 518–533**

doi: 10.1002/acn3.193

Abstract

Objective: Metachromatic leukodystrophy (MLD) is an autosomal recessive lysosomal storage disorder due to deficient activity of arylsulfatase A (ASA) that causes accumulation of sulfatide and lysosulfatide. The disorder is associated with demyelination and axonal loss in the central and peripheral nervous systems. The late infantile form has an early-onset, rapidly progressive course with severe sensorimotor dysfunction. The relationship between the degree of nerve damage and (lyso)sulfatide accumulation is, however, not established. **Methods**: In 13 children aged 2–5 years with severe motor impairment, markedly elevated cerebrospinal fluid (CSF) and sural nerve sulfatide and lysosulfatide levels, genotype, ASA mRNA levels, residual ASA, and protein cross-reactive immunological material (CRIM) confirmed the diagnosis. We studied the relationship between (lyso)sulfatide levels and (1) the clinical deficit in gross motor function (GMFM-88), (2) median and peroneal nerve motor and median and sural nerve sensory conduction studies (NCS), (3) median and tibial nerve somatosensory evoked potentials (SSEPs), (4) sural nerve histopathology, and (5) brain MR spectroscopy. **Results**: Eleven patients had a sensory-motor demyelinating neuropathy on electrophysiological testing, whereas two patients had normal studies. Sural nerve and CSF (lyso)sulfatide levels strongly correlated with abnormalities in electrophysiological parameters and large myelinated fiber loss in the sural nerve, but there were no associations between (lyso)sulfatide levels and measures of central nervous system (CNS) involvement (GMFM-88 score, SSEP, and MR spectroscopy). **Interpretation**: Nerve and CSF sulfatide and lysosulfatide accumulation provides a marker of disease severity in the PNS only; it does not reflect the extent of CNS involvement by the disease process. The magnitude of the biochemical disturbance produces a continuously graded spectrum of impairments in neurophysiological function and sural nerve histopathology.

Introduction

Metachromatic leukodystrophy (MLD) is an autosomal recessive disorder of lipid metabolism characterized by deficient activity of the lysosomal enzyme arylsulfatase A (ASA) with inability to degrade galactosylceramide-3-*O*-sulfate (sulfatide) and galactosylsphingosine-3-*O*-sulfate (lysosulfatide). Progressive accumulation of (lyso)sulfatide within oligodendrocytes and Schwann cells is associated with demyelination and axonal loss in the central (CNS) and peripheral nervous systems (PNS).[1] Of the three phenotypes of MLD (late infantile, juvenile, and adult–onset),

the late infantile form is most frequent and is usually diagnosed in the second year of life. The major presenting symptom is progressive gait abnormality with areflexic spasticity; death occurs during childhood.[2] In late infantile MLD, peripheral neuropathy often precedes the CNS manifestations of the disease and is characterized by severe slowing of motor and sensory conduction.[3,4] Studies of sural nerve histopathology in MLD have shown reduced large myelinated fiber density and accumulation of sulfatide within macrophages, Remak cells, and Schwann cells.

Since therapeutic approaches to MLD are being explored, we evaluated a wide range of potential markers of disease severity including biochemical and molecular analyses (ASA activity, genotype, ASA mRNA levels, and residual ASA CRIM), measurements of motor function (GMFM-88, gross motor function measure-88), brain MRI and MR spectroscopy, neurophysiological assessments and sural nerve biopsy. Particular emphasis was placed on cerebrospinal fluid (CSF) and sural nerve (lyso)sulfatide levels, as the relationship between severity of PNS and CNS impairment and extent of accumulation of sulfatide and lysosulfatide remains uncertain. We found strong correlations between (lyso)sulfatide levels, motor and sensory nerve function, and sural nerve histopathology and morphometry. There were no associations between these variables and measures of CNS dysfunction implying that disease burden in CNS and PNS are separable and discrete. We suggest that the severity of PNS axonal loss and demyelination is related to the toxic effects of tissue accumulation of sulfatide and lysosulfatide.[5]

Material and Methods

Study design and patient selections

The study presents exploratory analyses of the baseline data collected for a single center, open-label, nonrandomized, uncontrolled, Phase I clinical trial of intravenous enzyme replacement therapy in late infantile MLD (EudraCT 2006-005341-11, ClinicalTrials.gov identifier number NCT00418561). Thirteen children (Table 1), eight girls, and five boys, age range 25–59 months were enrolled. There were no screen failures. All of the children were referred between January and August 2007 from European clinics. Inclusion criteria were: (1) established diagnosis of MLD, (2) age between one and 5 years with onset of symptoms before age four, and (3) presence of residual voluntary motor function. Baseline evaluations provided the data for this report. They included clinical and motor function assessments, neuropsychological testing, nerve conduction studies (NCS) of the median, peroneal and sural nerves, median and tibial somatosensory evoked potentials (SSEPs), sural nerve biopsy with light and electron microscopic analyses, measurement of CSF sulfatide and sural nerve sulfatide and lysosulfatide concentrations, determination of relative ASA mRNA expression level, estimation of ASA CRIM (cross-reactive immunological material), and MR spectroscopy studies with measurement of *N*-acetylaspartate levels (NAA) in the centrum semiovale. Since there was a broad spectrum of motor dysfunction, the children were representative of a cross-sectional sample of the late infantile MLD population in the specified age range.

Table 1. Demographic data, clinical features, and mutations in 13 children with late infantile MLD.

Patient ID	Gender	Age (months)	Mutation 1	Mutation 2	Clinical features	GMFM-88 score
1	Female	30	c.459+1G>A	c.459+1G>A	Able to walk, unsteady	180
2	Female	51	c.392_403del	c.1171A>G;p.S391G (in combination with rs743616)	Able to sit, grabs toys	36
3	Male	31	c.459+1G>A	c.1304C>G;p.P435R	Unable to sit, moves head	13
4	Male	34	c.287C>T;p.S96F	c.459+1G>A	Unable to sit, moves head	15
5	Male	44	c.296dupG	c.1217_1225del	Unable to sit, moves head	25
6	Female	36	c.459+1G>A	c.730C>T;p.R244C	Unable to sit, moves head	21
7	Female	41	c.635C>T;p.A212V	c.635C>T;p.A212V	Able to walk, slight spasticity, slightly impaired motor function	131
8	Male	59	c.459+1G>A	c.602A>G;p.Y201C	Able to sit, grabs toys	38
9	Female	26	c.459+1G>A	c.1240T>C;p.C414R	Unable to sit, moves head	47
10	Female	40	c.731G>A;p.R244H	c.919G>A;p.E307K	Unable to sit, moves head	18
11	Male	34	c.459+1G>A	c.459+1G>A	Unable to sit, moves head	21
12	Female	25	c.443C>T;p.P148L	c.443C>T;p.P148L	Able to walk and run	141
13	Female	37	c.459+1G>A	c.973+1G>A	Unable to sit, moves head	34

MLD, metachromatic leukodystrophy.

Standard protocol approval, registration and patient consent

The clinical study was approved by the Ethical Committee of Copenhagen. Written informed consent was obtained. Control sural nerve samples for biochemical (eight adult) and morphometric (three children) analyses were obtained from patients who underwent diagnostic evaluation for suspected neuromuscular disorders at Johns Hopkins Medical Institutions. Patients consented to use of portions of the biopsy specimens for research purposes. The amplitudes of sensory nerve action potentials (SNAP) and detailed histological analyses were normal for all control patients.

Motor function evaluation (GMFM-88)

A physiotherapist specialized in child development examined motor function using the GMFM-88, which records motor skills that are typical of normal development (Table 1). The test is validated to evaluate children with neurological disorders.[6,7]

Molecular analyses

Genomic DNA was isolated from whole blood using a standard salting out method,[8] and the entire coding and intronic sequence of ASA were amplified by PCR and sequenced directly in a diagnostic setting (primers and PCR conditions are available upon request, Table 1).

Quantitation of ASA mRNA

Total RNA was isolated from cultured fibroblasts from the patients and normal donor controls using RNeasy (Qiagen, Copenhagen, Denmark), and cDNA was generated using Superscript II™ (Invitrogen, Life Technologies Europe BV, Naerum, Denmark) in combination with random hexamer primers, both according to the manufacturer's description. Quantitative real-time PCR (qPCR) was performed with cDNA-specific primers for ASA (exon 4–5) and the human 18S locus in combination with florescent-marked TaqMan probes. The relative amount of target ASA mRNA was normalized to 18S rRNA and expressed as a percentage of healthy control values using the $\Delta\Delta$CT method[9] (primer and probe sequences are available upon request Table 2).

ASA CRIM in fibroblasts

Fibroblasts from skin biopsies of MLD patients enrolled in the clinical trial were harvested and expanded at the clinical site. Control fibroblast cell lines from normal donors were obtained from Coriell Cell Repositories (Camden, NJ, USA) they were expanded in Dulbecco's Modified Eagle Medium (DMEM) supplemented with 10% fetal bovine serum and harvested by trypsinization. Cell lysates were prepared by homogenizing cells in lysis buffer (10 mmol/L Tris pH 7 containing 0.1% triton X-100 $\pm$ 1× protease inhibitor cocktail) (Roche Catalogue No. 04693159001); lysates were stored at ≤ -65°C until analysis. ASA CRIM in cell lysates was determined by ELISA with a paired

Table 2. Biomarkers in 13 patients with late infantile MLD.

Patient ID	%mRNA ASA	CRIM (ng/mg)	SN sulfatide (ng/mg dw)[1]	SN lysosulfatide (ng/mg dw)[2]	CSF sulfatide (nmol/L)	NAA in CS
1	16.2	0.04	7670	5.32	ND	2.65
2	48.1	0.28	3430	1.48	200	0.63
3	35.7	0.31	5630	1.99	750	0.28
4	18.5	0.03	7620	1.18	550	0.59
5	28.3	0.58	No SN	No SN	1450	0.74
6	ND	ND	4700	2.47	2300	0.35
7	45.9	0.09	3800	0.65	700	1.20
8	15.9	0.11	2160	0.53	225	1.42
9	20.1	0.92	9530	8.50	1200	0.87
10	34.6	0.02	7850	4.94	2200	0.42
11	6.0	0.10	11,300	9.85	1930	1.04
12	4.9	0.02	7190	ND	1150	2.34
13	3.0	0.04	9400	2.73	675	0.55
NV	100	73.57	935 $\pm$ 157	0.14 $\pm$ 0.12	<50	3.49 $\pm$ 0.39

MLD, metachromatic leukodystrophy; ASA, arylsulfatase A; CRIM, cross-reactive immunological material; SN, sural nerve; dw, dry weight; CSF, cerebrospinal fluid; NAA, *N*-acetylaspartate; CS, centrum semiovale; No SN, no sural nerves; ND, not done; NV, normal values.

[1]Of the 19 molecular species monitored during LC-MS/MS: liquid chromatography–tandem mass spectrometry analysis of sural nerve sulfatide, the four most abundant species on a mass basis are C24:1 (23%), C24:0 (20%), C24:0-OH (9%), and C22:0 (7%); the distribution in MLD and control nerves is similar. C24:1 sulfatide has a molecular weight of 889.

[2]Lysosulfatide has a molecular weight of 541.

polyclonal goat anti-ASA antibody (R&D system, AF2485, BAF2485, Minneapolis, MN, USA) followed by detection of bound ASA CRIM with streptavidin-horseradish peroxidase and TMB peroxidase substrate. Cell lysates from MLD patients were tested at 1:5 and 1:10 dilution, whereas lysates from controls were tested at 1:50 dilution. ASA concentration in cell lysates (ng/mL) was calculated based on the calibration curve of recombinant human ASA in the same assay. Protein concentrations of cell lysates were determined by Pierce™ Life Technologies (Rockford, IL, USA) BCA protein assay kit according to the manufacturer's instructions; results are reported as ng ASA CRIM/mg total protein (Table 2).

LC-MS/MS analysis of sural nerve sulfatide and lysosulfatide

Tissue samples (~2–10 mg of wet weight) were weighed, dried, and homogenized in 1 mL of water using a 24-bead homogenizer. An aliquot of the homogenate equivalent to ~0.2 mg of dry tissue was used for analysis. Briefly, after adding C12:0 sulfatide (Avanti Polar Lipids, Alabaster, AL) as the internal standard (ISTD), samples were extracted with acetonitrile, subjected to alkaline hydrolysis in 4 N sodium hydroxide, quenched with acetic acid, and then further purified by solid phase extraction (SPE) (Oasis WAX 1 mL cartridge; Waters, Milford, MA). The eluate from SPE was dried under nitrogen and the residue was reconstituted in 200 μL of methanol prior to LC-MS/MS analysis (Table 2).

Calibration curve standards and quality control samples were prepared by spiking cynomolgous monkey sural nerve homogenate with C16:0 sulfatide (analyte; Matreya, Pleasant Gap, PA) in the range of 20–2000 ng/mg of dry tissue and 400 ng/mg of C12:0 sulfatide (ISTD, Avanti Polar Lipids).

Sample preparation for lysosulfatide detection followed the same extraction procedure, except that acetonitrile/methanol (1:1 v/v) was used as the extraction solvent, and neither alkaline hydrolysis nor SPE were carried out. To generate the standard curve, cynomolgous monkey sural nerve homogenate was spiked with lysosulfatide as the analyte (Matreya) in the range of 0.3–17 ng/mg of dry tissue and 5 ng/mg of C2:0 sulfatide as ISTD (Matreya).

Control values for sural nerve lysosulfatide and sulfatide concentration were determined by analysis of glutaraldehyde-fixed nerves from eight adult patients (age 37–61; 7F/1M) who underwent biopsy at Johns Hopkins Medical Institutions for suspected neuromuscular disorders. Pilot experiments demonstrated that sulfatide and lysosulfatide levels in cynomolgous monkey sural nerves were comparable in freshly harvested and glutaraldehyde-fixed tissue.

For quantitation of sulfatide species, a 10-μL aliquot of reconstituted sample was injected onto an XBridge BEH 300 2.1 × 50 mm reversed-phase C4 column (3.5 μm particle size, Waters) connected to an Accela HPLC system (Thermo Electron, San Jose, CA). Elution was performed using a linear gradient from 40% 2 mmol/L aqueous ammonium formate: 60% acetonitrile to 100% acetonitrile (pH 8.5) over 5 min at a flow rate of 0.5 mL/min. The eluent from the column was introduced into a triple quadrupole mass spectrometer operated in negative-ion electrospray mode (TSQ Quantum Ultra; Thermo Electron). Sulfatide species were identified by precursor ion scan for *m/z* 97 (the most abundant fragment ion). The monitored SRM transitions were *m/z* 722 (for the ISTD), 778, 804, 806, 822, 832, 834, 850, 860, 862, 874, 876, 878, 886, 888, 890, 902, 904, 906, and 916. Calibration curves were constructed by linear regression analysis of the peak area ratios of C16:0/C12:0 versus the amount of C16:0 sulfatide. Sulfatide concentration was calculated from the summed values of each of the 19 molecular species.

For quantitation of lysosulfatide, the same LC-MS/MS system was used. The solvent gradient consisted of water/acetonitrile each containing 5 mmol/L of ammonium formate ramped from 20 to 100% acetonitrile over 5 min at a flow rate of 0.4 mL/min. The SRM transitions monitored for lysosulfatide and the ISTD C2:0 sulfatide were *m/z* 540 to *m/z* 97 and *m/z* 582 to *m/z* 97, respectively.

CSF sulfatide

CSF sulfatide was determined by immunostaining of thin-layer chromatograms with the Sulph I antisulfatide antibody as previously described (Table 2).[10,11]

Proton MRSI studies

Magnetic resonance spectroscopy imaging (MRSI) was performed under general anesthesia utilizing standard institutional scanning protocols. Echo-planar spectroscopic imaging provided multislice metabolic maps covering deep white matter from which centrum semiovale NAA levels were measured as previously described (Table 2).[12]

Nerve conduction studies

The children were sedated with chloral hydrate rectally (30–50 mg/kg body weight) and temperature of the limbs was kept at 35–38°C using a thermocoupled infrared heating lamp. Motor fibers of the right median nerve were stimulated supramaximally at the wrist and elbow through surface electrodes. The compound muscle action potential (CMAP) was recorded through a surface electrode placed

over the abductor pollicis brevis (APB) muscle. The CMAPs were amplified (frequency range 20 Hz–10 kHz) and latencies and amplitudes were measured off-line. The distal motor latency (DML) from wrist to APB was measured and the motor nerve conduction velocity (MNCV) from elbow to wrist calculated. F-waves were recorded by stimulating the median nerve at the wrist and the shortest latency was measured. Sensory fibers in digit 2 were stimulated supramaximally through ring surface electrodes. The orthodromic compound SNAP was recorded through surface electrodes at the wrist and amplified (frequency range 200 Hz–4 kHz); amplitudes were measured peak-to-peak. The sensory nerve conduction velocity (SNCV) from digit 2 to wrist was calculated (Table 3).

Motor fibers of the right peroneal nerve were stimulated supramaximally at the ankle and fibular head. The CMAP was recorded from the extensor digitorum brevis muscle (EDB). The DML from ankle to EDB was measured, and the MNCV from the fibular head to ankle was calculated. F-waves were recorded by stimulating the peroneal nerve at the ankle.

Both sural nerves were stimulated supramaximally at the lateral malleolus through insulated needles with a 3-mm bared tip. The orthodromic SNAP was recorded unipolarly through a needle electrode placed close to the nerve at midcalf and referenced to a needle placed medially at a transverse distance of 2 cm, amplified (frequency range of 200 Hz–4 kHz) and averaged in two runs to ensure reproducibility. Latency to the first positive phase was measured and the SNCV calculated. The amplitude was measured peak-to-peak (Fig. 1).

Motor and sensory conduction study values were compared to our own laboratory controls[13] and other published values[14] in normal children (Table 3). In normal children, there is a gradual increase in MNCV and decrease in DML with age from birth to 3–4 years at

Table 3. Electrophysiological studies in 13 patients with late infantile MLD.

	Median nerve conduction studies					Peroneal nerve conduction studies			Sural nerve conduction studies		Median SSEP	Tibial SSEP
Patient ID	CMAP (mV)[1]	DML (msec)[2]	MNCV (m/sec)[3]	SNAP (μV)[4]	SNCV (m/sec)[5]	CMAP (mV)[6]	DML (msec)[7]	MNCV (m/sec)[8]	SNAP (μV)[9]	SNCV (m/sec)[10]	N20 (msec)[11]	P28 (msec)[12]
1	7.0	5.7	23	5.4	46	0.9	8.2	19	12.4	38	21.4	50.7
2	5.2	3.5	27	2.8	33	5.1	5.1	34	5.7	24	17.0	36.0
3	3.5	5.8	16	2.2	18	1.3	7.2	17	0.5	27	25.4	54.9
4	7.1	5.3	13	1.4	34	2.8	7.9	14	1.2	33	23.6	45.6
5	8.2	8.0	11	1.1	24	0.7	9.5	10	ND	ND	38.5	88.6
6	5.5	6.6	12	1.6	20	3.0	8.2	11	2.3	16	33.7	113.5
7	7.5	3.4	47	21.1	54	4.3	4.5	46	100.9	52	17.2	34.7
8	11.2	2.7	48	26.6	53	9.2	3.2	49	97.5	51	15.7	56.2
9	4.2	6.4	19	1.9	19	1.8	7.6	23	4.2	34	23.1	46.0
10	5.1	5.8	13	1.7	12	0.2	10.3	9	NR	NR	NR	NR
11	2.9	7.7	10	0.8	16	1.5	11.6	10	0.1	18	28.2	39.3
12	5.2	4.7	23	2.6	40	1.6	6.3	16	1.9	43	19.8	46.7
13	8.9	5.3	17	0.7	33	4.0	7.7	16	0.3	33	26.5	37.0
NV	2–10	2–3	40–60	5–15	50–60	1–7	2–3	42–52	>19	45–55	13–17	24–33

MLD, metachromatic leukodystrophy; SSEP, somatosensory evoked potential; CMAP, compound muscle action potential; DML, distal motor latency; MNCV, motor nerve conduction velocity; SNAP, sensory nerve action potential; SNCV, sensory nerve conduction velocity; ND, study not done; NR, no response; NV, normal values (ranges in children aged 2–5 years[13,14]).

[1]Compound muscle action potential from abductor pollicis brevis muscle (APB).

[2]Distal motor latency from wrist to APB.

[3]Motor nerve conduction velocity from elbow to wrist.

[4]Compound sensory action potential (SNAP) from digit 2 to wrist.

[5]Sensory nerve conduction velocity from digit 2 to wrist.

[6]Compound muscle action potential from extensor digitorum brevis muscle (EDB).

[7]Distal motor latency from ankle to EDB.

[8]Motor nerve conduction velocity from fibular head to ankle.

[9]Sural nerve SNAP from lateral malleolus at midcalf.

[10]Sensory nerve conduction velocity from lateral malleolus to midcalf.

[11]Latency of median nerve somatosensory evoked potential from wrist to cortex.

[12]Latency of tibial nerve somatosensory evoked potential from medial malleolus to cortex.

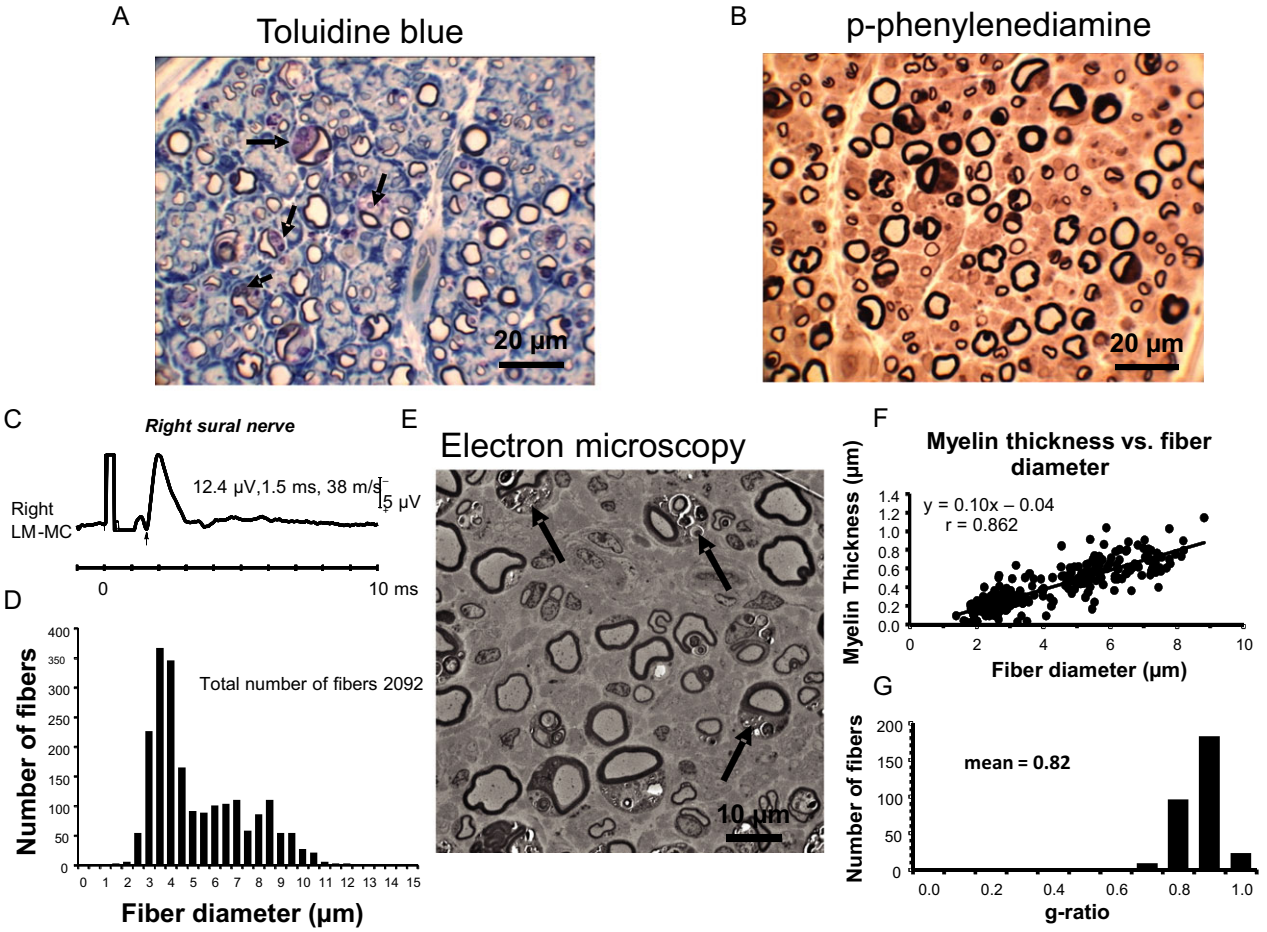

Figure 1. Composite of light microscopy semithin sections stained with toluidine blue (A, arrows indicate metachromatic granules) and p-phenylenediamine (B) and ultrathin sections (E) from the right sural nerve of a 2.5-year-old girl with late infantile metachromatic leukodystrophy (MLD) (patient 1). The diameter distribution of myelinated fibers and the calculated total number from light microscopy are shown below left (D). The myelin versus fiber diameter relationship (F) and the *g*-ratio distribution (G) were obtained from the electron micrographs. The morphological data were compared to the nerve conduction studies of the same sural nerve (C).

which time the MNCV is similar to young adults. The increase in conduction velocity in normal children from 2 to 5 years of age is in the order of 5–10%.[12] The amplitude of the CMAP increases slightly from birth to adulthood. SNCV of the median and sural nerves increases with age from birth to 3 years of age at which time the SNCV is similar to young adults. The amplitudes of the SNAPs recorded from the median and sural nerves increase gradually to adult values by 3 years of age.

Somatosensory evoked potentials

Bilateral median and tibial nerve SSEPs were examined. Stimulation of the median nerve through surface electrodes at the wrist was adjusted to elicit a movement of the thumb whenever possible. Surface electrodes were placed over the median nerve at the elbow and supraclavicular fossa (Erb's point) to record the nerve action potential. Surface electrodes were placed over the C7 spinous process to record the spinal response and over the contralateral C3/C4 cranial site to record the cortical response. The tibial nerve was stimulated through surface electrodes at the medial malleolus. Surface electrodes were placed at the popliteal fossa to record the nerve action potential, over the T12 spinous process to record the spinal response, and over the vertex at Cz to record the cortical response. The latencies were compared to published values from normal children (Table 3).[15–17]

Pathology of sural nerve

Right sural nerve biopsies were examined in 12 children. The nerves were fixed by immersion in glutaraldehyde (2.0% in 0.1 mol/L cacodylate buffer) for 24 h. Fixed

Table 4. Morphometric values from sural nerves of 12 patients with late infantile MLD.

Patient ID	Total number of fibers	Number fibers >7 μm	Percent fibers >7 μm	Number fibers >9 μm	Percent fibers >9 μm	Mean diameter of 10 largest fibers (μm)	Mean axon diameter (μm)	Mean myelin thickness (μm)	Mean *g*-ratio	Myelin-fiber slope[1]
1	2092	536	26	172	8	11.5	3.3	0.39	0.82	0.10
2	4735	839	18	102	2	10.3	3.1	0.33	0.83	0.10
3	3591	399	11	9	0	8.8	2.0	0.23	0.82	0.13
4	4050	871	21	120	3	10.0	2.3	0.27	0.80	0.08
5[2]	ND	ND	ND	ND	ND	ND	ND	ND	ND	ND
6	1587	188	12	3	0	8.5	3.3	0.29	0.85	0.08
7	5051	1820	36	637	13	12.0	3.2	0.43	0.79	0.12
8	6400	1947	30	867	14	11.5	2.6	0.37	0.78	0.13
9	5010	1166	23	159	3	10.0	2.8	0.29	0.83	0.09
10	1829	165	9	5	0	8.5	3.0	0.32	0.82	0.07
11	5020	255	5	0	0	8.0	3.0	0.29	0.83	0.09
12	3230	614	19	55	2	9.5	3.1	0.29	0.84	0.07
13	6160	501	8	0	0	9.0	3.0	0.30	0.84	0.13
NV	7422–9397	>1800	>25	>400	>5	10.0–12.5	2–3	0.68–1.20	0.65	0.13–0.23

MLD, metachromatic leukodystrophy; ND, study not done; NV, normal values.
[1]Slope of myelin thickness (μm) versus fiber diameter (μm).
[2]Sural nerve was previously biopsied in connection with diagnosis at another institution; not included in the present study.

nerves were postfixed in 1% osmium tetroxide in 0.1 mol/L Sørensen′s buffer, dehydrated in graded alcohol (30–100%), cleared in propylene oxide, and embedded in increasing concentrations of epoxy resin until polymerized in pure epon in a heated cabinet. Cross sections of the sural nerve were cut with dry glass knives at 2–3 μm thickness, overstained with p-phenylenediamine, mounted and investigated with a light microscope (Olympus BX51; Olympus Danmark A/S, Ballerup, Denmark). Transverse sections were stained with toluidine blue to assess the presence of metachromatic inclusions in Schwann cells and macrophages. Studies in the MLD patients were compared with three control children aged 2, 3, and 11 years examined at Johns Hopkins Medical Institutions to exclude giant fiber neuropathy (Table 4).

Light microscopic examination

Overview micrographs at 40× and detailed micrographs at 100× were photographed with a digital camera (Olympus DP71), and images were processed using the MNERVE custom made nerve morphometry software developed at MATLAB (Version 2010a; MathWorks, Inc., Natick, MA). The total nerve area was traced from the overview micrographs and myelin rings were traced from at least 10% of the total nerve area; fiber diameters were calculated as the diameter of the circle having the same area as the outer contours of the "myelin rings." Fiber density within the measured area was then used to calculate the total number of myelinated fibers (Fig. 1).

Electron microscopic evaluation

For ultrastructural analyses, 70-nm thick cross sections of the nerves were obtained and stained with citrate/uranyl acetate. Five to seven electron micrographs at 2000× were acquired from each nerve using a Hitachi 7600 electron microscope (Hitachi 7600 TEM, Tokyo, Japan). A micrograph was taken from each fascicle within the nerve. Measurements of the outer and inner diameters of the myelin sheath were obtained from 150 to 400 fibers to obtain the axon and fiber diameters as described above. The *g*-ratio and the myelin thickness were calculated from the diameters (Fig. 1).

Data analysis

The goal of this exploratory analysis was to assess important associations between a broad range of disease biomarkers in a cross-sectional sample of 13 children with late infantile MLD. In addition, sural nerve samples were obtained from three control children for morphometric analyses. Due to the small sample size, model building and statistical comparisons between the MLD and control patients were not appropriate. Therefore, the exploratory analyses were only descriptive in nature. A measure of the linear association between two variables was obtained using Pearson correlation. The resulting estimates were tested for statistical significance at the 0.05 level; *P*-values were not adjusted for multiplicity. Correlation estimates for the SNAP amplitudes were obtained after logarithmic

transformation based on previous studies.[18] Empirical cumulative distributions plots were produced to contrast the *g*-ratio data between the MLD patients and the three controls.

Results

Demographic, clinical and genotypic characteristics

All 13 children (Table 1) had pathologically low leukocyte ASA enzymatic activities (2.2–9.4 nmol/h per mg cell protein; normal >20 nmol/h per mg cell protein) and elevated urinary sulfatide excretion. They all presented before age 4 with progressive symptoms of late infantile MLD including spasticity, impaired gait, late motor milestones, or evidence of cognitive impairment. On motor function evaluation, three children were able to walk (GMFM-88 scores: 131–180), two were able to sit without support (GMFM-88 scores: 36–38), and eight were unable to sit (GMFM-88 scores: 13–47); the maximum normal score is 264. The abnormalities observed on NCS did not correlate with CNS disease burden as measured by motor function assessment (GMFM-88) and NAA levels in the centrum semiovale.

The diagnosis of MLD was confirmed by molecular analysis (Table 1). Fifteen different mutations were identified; the common c.459+1G>A splice site mutation, which is frequent in the late infantile phenotype,[19] accounted for 38% of the alleles (10/26). Nine of the 13 patients carried at least one allele predicted to be targeted by the nonsense mediated mRNA decay pathway (NMD) due to a disrupted reading-frame. Three novel mutations were identified (c.1171A>G, c.1240T>C, and c.1304C>G) and will be described in detail elsewhere. All novel mutations were identified in a compound heterozygous state with a known pathogenic mutation. Patients 4, 5, and 13 were in addition heterozygous for the pseudo-allele (c.*96A>G), whereas patient 12 was homozygous. Overall, mutation analysis confirmed the association of splice site and frame shift mutations with the late infantile phenotype.[1]

Quantitation of ASA mRNA

The relative amount of ASA mRNA varied from 3.0% (Pt 13) to 48.1% (Pt 2) compared to control values, which may be explained in part by the genotype of the individual patients (Tables 1, 2). Except for Pt 12, patients carrying one or two alleles predicted to undergo NMD exhibited the lowest expression levels. Examination of arylsulfatase CRIM levels in fibroblasts obtained from skin biopsies showed that all patients had extremely low values (<1 ng/mg) compared to the control reference value (74 ng/mg); there was no apparent relationship between CRIM levels and other measures of disease severity.

Analysis of (lyso)sulfatides in CSF and sural nerve

CSF sulfatide varied from 200 to 2300 nmol/L (normal <50 nmol/L). The two oldest patients (two and eight) had the lowest values (200 and 225 nmol/L); no relationship between disease course, age, motor function or central white matter NAA levels, and the amount of sulfatide in spinal fluid was apparent (Table 2). The patients who were still able to walk had values of 700 and 1150 nmol/L.

Sural nerve sulfatide concentration was increased 2- to 12-fold (2160–11,300 ng/mg dry weight) compared with normal values (Table 2); lysosulfatide levels were increased 4- to 70-fold (0.53–9.85 ng/mg dry weight), and the two concentrations were strongly correlated ($P < 0.005$). The correlation between CSF sulfatide and sural nerve sulfatide concentration did not reach statistical significance ($P = 0.1$), whereas the correlation between CSF sulfatide and sural nerve lysosulfatide was significant ($P < 0.02$).

Proton MRSI findings

NAA provides a marker of neuronal and axonal integrity. Inspection of cerebral NAA maps revealed marked signal attenuation in the deep white matter (centrum semiovale) compared to findings in normal controls (Table 2). We have previously reported a significant relationship between progressive attenuation of the NAA signal and loss of motor function in this cohort.[12] Central white matter NAA levels did not correlate with CSF or sural nerve (lyso)sulfatide concentrations, molecular measurements (ASA mRNA expression levels and CRIM), neurophysiological parameters, or sural nerve pathology.

Electrophysiological findings

Nerve conduction studies

NCS of the sural, median, and peroneal nerves revealed pronounced abnormalities of sensory and motor fibers in 11 patients, whereas two patients had normal values (Table 3). In normal children the stimulus strength required to obtain maximal responses is <20 mA, but in patients with MLD the threshold was often markedly increased requiring stimulus strengths of 50–100 mA and prolonged duration above the usual 0.2 msec to ensure supramaximal stimulation.

The median nerve DMLs in 11 children with neuropathy were 40–220% prolonged and near normal in two patients (Fig. 2) (normal range 2–3 msec[14]). The median MNCVs

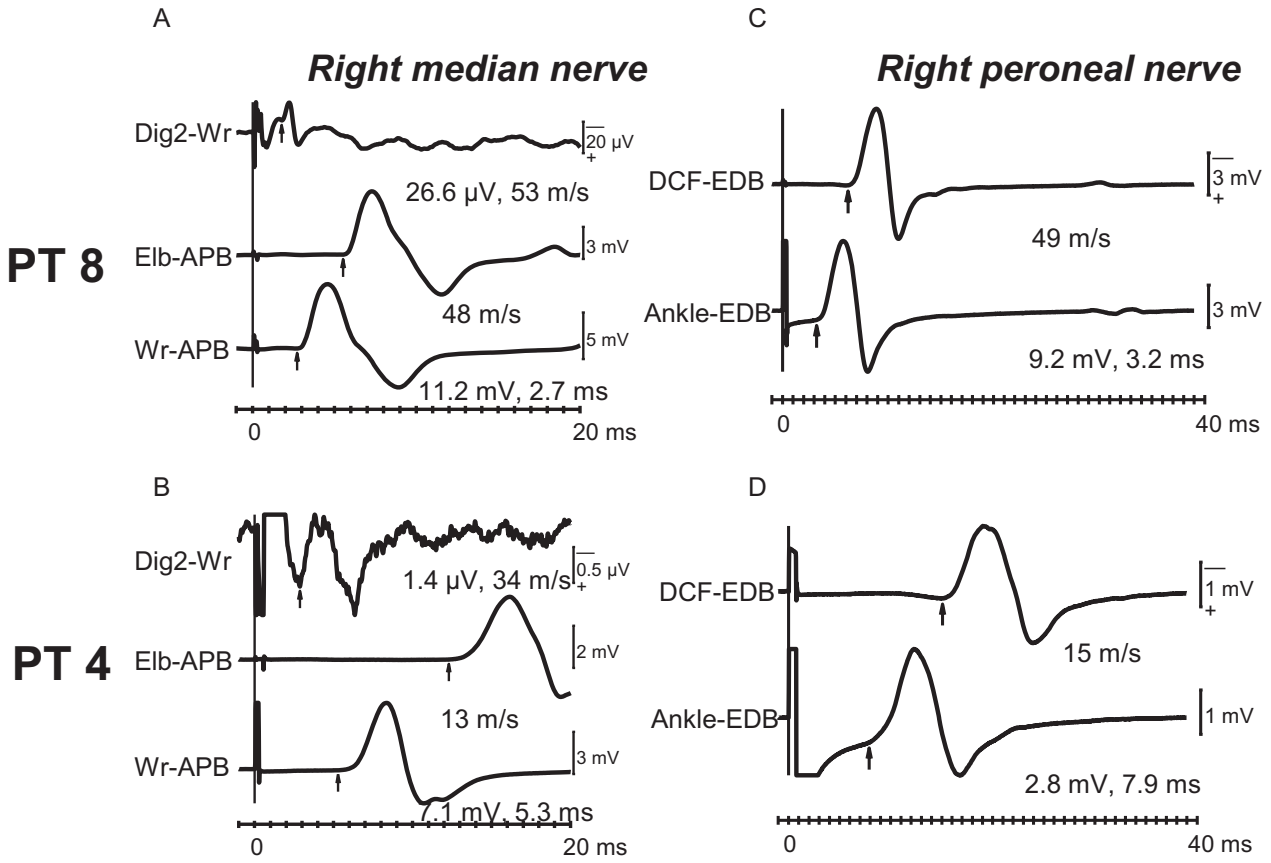

Figure 2. Motor and sensory nerve conduction studies from the right median nerve (A and B, left column) and motor conduction studies from the right peroneal nerve (C and D, right column). The patient on top (A and C) was a 5-year-old boy (patient 8) without electrophysiological evidence of neuropathy, and the patient below (B and D) was a 3-year-old boy with severe demyelinating neuropathy (patient 4). The compound sensory nerve action potential (SNAP) of the median nerve was evoked by stimulation at Digit2 (Dig2) and recording at the wrist (Wr), the compound muscle action potential (CMAP) of the median nerve was evoked by stimulation at wrist (Wr) and elbow (Elb) and recorded at the abductor pollicis brevis muscle (APB). The CMAP of the peroneal nerve was evoked by stimulation at the ankle and distal to the fibular head (DCF) and recorded from the extensor digitorum brevis muscle (EDB). Latencies, conduction velocities, and amplitudes of SNAPs and CMAPs are indicated below traces.

were 46–78% reduced in 11 patients and normal in two (normal values in children aged 2–4 years, 45–55 m/sec[13,14]). The F-wave latencies were prolonged at 28–75 msec in nine and normal in two patients; F-waves were absent in two patients (normal range 15–20 msec[14]). The amplitudes of the CMAPs evoked at the wrist were within normal range in all patients (Fig. 2, Table 3) and when evoked at the elbow were 31 ± 5% smaller than at the wrist. The orthodromic median nerve SNCVs from digit 2 to wrist (Table 3) were 9–76% reduced in 11 and normal in two patients; SNAP amplitudes were 76–93% reduced in 10 and normal in three (Fig. 2).

The peroneal nerve DMLs were 104–364% prolonged in 11 children and near normal in two. The MNCVs were 15–78% reduced in 11 patients and normal in two (Fig. 2, Table 3). F-waves could only be recorded in two patients with abnormal NCS and were markedly prolonged at 57 and 73 msec; they were normal in two patients with normal NCS (normal range 25–35 msec[20]). The amplitudes of the CMAPs evoked at the ankle were reduced in three patients and within normal range in 10 patients (Table 3); when evoked at the fibular head they were 21 ± 8% smaller than at the ankle.

The *sural nerve* SNAPs were absent in one patient, reduced by 75–99% in nine, and normal in two patients. The SNCVs were reduced by 17–47% in nine and normal in two patients (Fig. 3).

In order to ascertain the variability in conduction abnormalities in the tested nerves, correlations between amplitudes, latencies and conduction velocities were examined. The amplitudes of CMAPs and logSNAPs were linearly correlated ($r = 0.522$, $n = 24$, $P < 0.01$) as were the MNCVs and the SNCVs ($r = 0.797$, $n = 24$, $P < 0.0005$). The DMLs and MNCVs of the peroneal and median

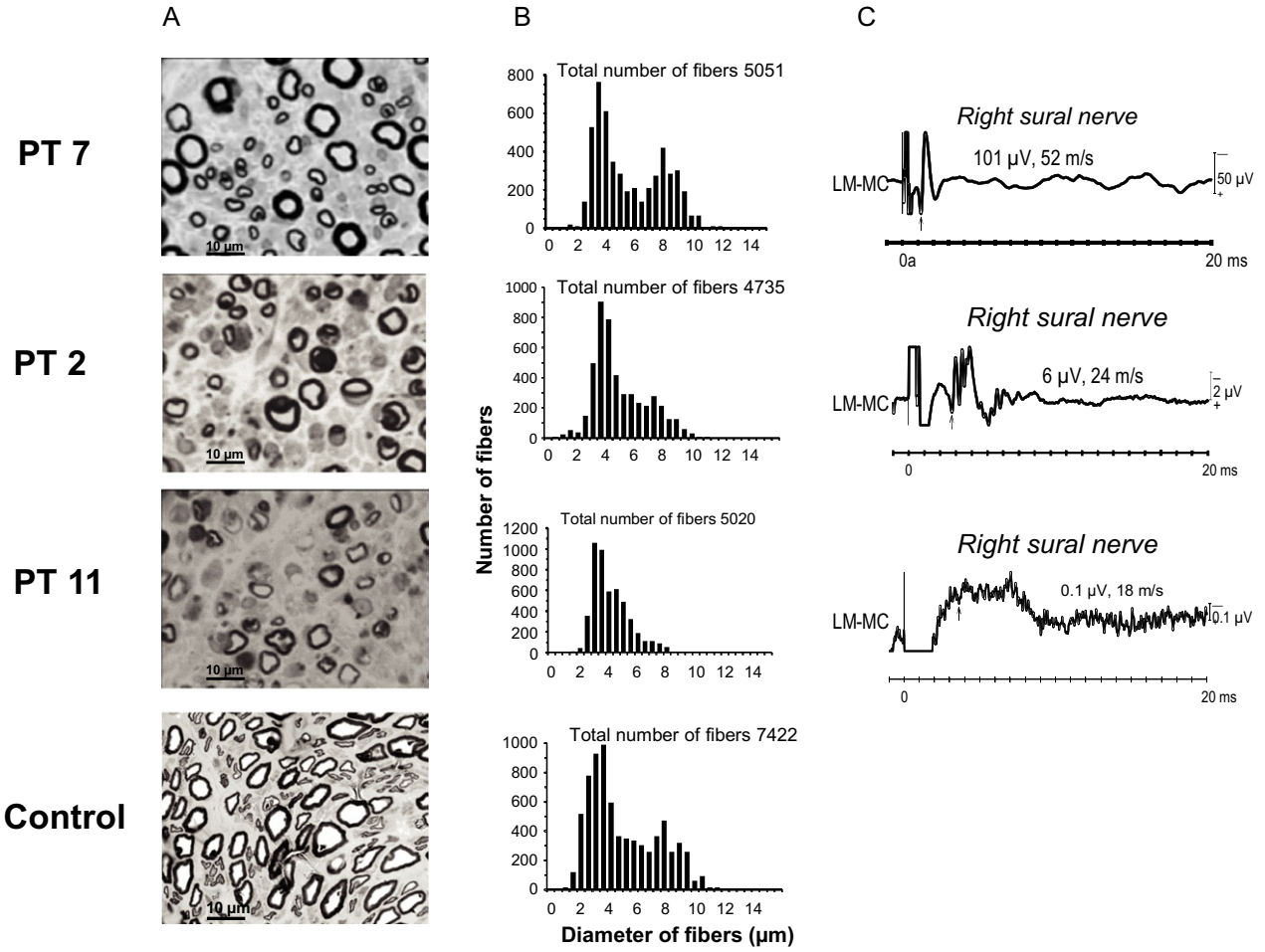

Figure 3. Comparison of morphological (A and B) and electrophysiological (C) findings of the right sural nerves in three patients with late infantile metachromatic leukodystrophy (MLD). The three patients had either no evidence of neuropathy (top, 3-year-old girl, patient 7), moderate neuropathy (above middle, 4-year-old girl, patient 2), or severe neuropathy (below middle, 4-year-old boy, patient 11). The lowermost section was from a 3-year-old control without evidence of neuropathy. The diameter distribution and total number of fibers (B, center column) were calculated from light microscopy of p-phenyldiamine semithin sections. Sural nerve conduction studies are shown in the right column (C). The amplitudes and conduction velocities are indicated above the traces.

nerves were linearly correlated ($r = 0.898$–0.966, $n = 13$, $P < 0.0005$) as were the CMAP amplitudes ($r = 0.634$; $n = 13$, $P = 0.02$). Similarly, the SNCVs of the sural and the median nerves were linearly correlated ($r = 0.870$, $n = 11$, $P < 0.0005$) as were the logSNAP amplitudes ($r = 0.904$, $n = 11$, $P < 0.005$).

Somatosensory evoked potentials

Cortical responses to median and tibial nerve stimulation could be recorded in 12 of the 13 patients. The median nerve SSEPs had prolonged latencies (range 19.8–38.5 msec) to N20 in nine patients, they were borderline in two, and normal in one patient (Table 3). The tibial nerve SSEPs had prolonged latencies (range 35–114 msec) to P28 in all 12 patients. The central conduction times with median nerve stimulation could be ascertained in 10 patients in whom an N13 response could be recorded at C7, and they were found to be abnormal in nine. With tibial nerve stimulation, the central conduction times could only be ascertained in four patients, and they were abnormal in all.

Morphometric analysis of sural nerve biopsies

Light and electron microscopic studies of sural nerve biopsies from 12 patients were compared with findings in three control sural nerves from children aged 2, 3, and 11 years and with values referenced in the literature.[21,22] The total number of myelinated fibers ranged from 1587

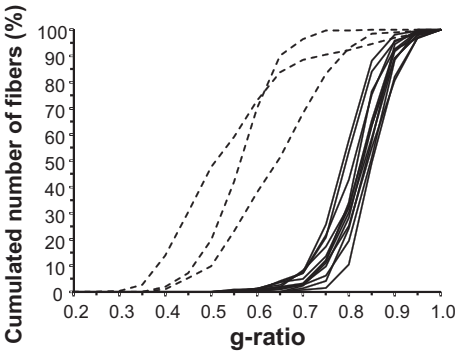

Figure 4. Cumulative distributions of *g*-ratios from sural nerves in 12 patients with late infantile metachromatic leukodystrophy (full lines) and three children without neuropathy (stippled lines).

to 6400 and was lower than normal in all patients compared with the values from three control children (7422–9397); the number of large fibers >7–9 μm was reduced in 10 patients. The fiber distribution was bimodal in five and unimodal in seven patients (Fig. 3); the diameter of the 10 largest fibers in the patients' nerves ranged between 8 and 12 μm and were smaller than control in six and within normal range in six patients. Average axonal diameters were similar in the patients and controls, whereas myelin thickness, *g*-ratio, and the slope of myelin thickness versus fiber diameter plots in control nerves differed substantially from the patient values. Cumulative *g*-ratio plots showed complete separation between control and MLD nerves consistent with evidence of thinned myelin in all patients (Fig. 4, Table 4).

Relationship between electrophysiological and morphometric results

The sural and median nerve SNAP amplitudes were closely related to the number of myelinated fibers ≥7–9 μm in diameter ($r > 0.8$, $P < 0.001$, Fig. 5A) and to the diameters of the 10 largest fibers in the sural nerve ($r = 0.88$, $P < 0.001$, Fig. 5B), whereas there was no correlation with the total number of myelinated fibers. Moreover, the maximal median and sural SNCVs were closely related to the number of large myelinated nerve fibers ($r = 0.82$, $P < 0.005$). Factors in addition to the number of large myelinated fibers contributed to reduction in SNCV. The relationship between maximum SNCV and the diameter of the 10 largest fibers in normal sural nerves (conversion factor of 4.3 m/sec per μm)[23] could not be applied to the sural nerves of the patients (Fig. 5C). SNCV as a function of fiber diameter was less than expected for the patients, which indicates that demyelination contributed to the slowing of conduction.

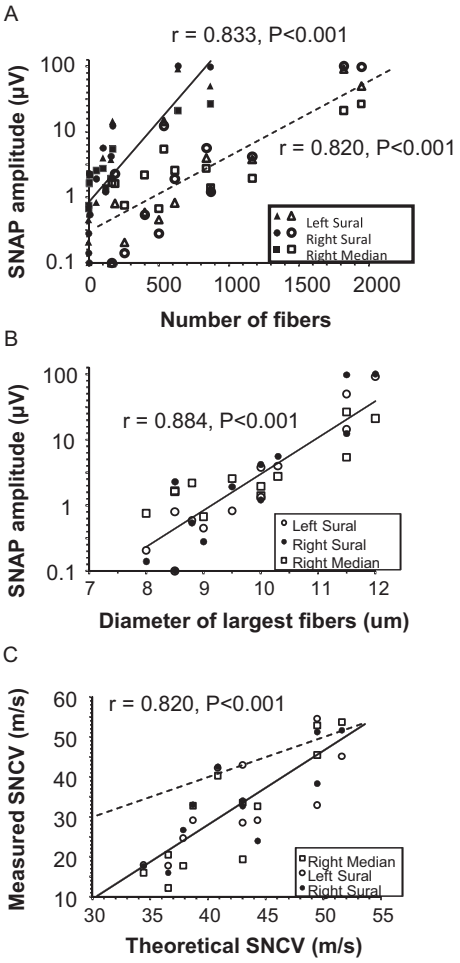

Figure 5. Relationships between sensory nerve action potentials (SNAP) and sural nerve myelinated fibers in patients with metachromatic leukodystrophy. (A) The SNAP amplitudes from the median nerve, the left sural nerve, and right sural nerves were correlated with the number of fibers with diameters above 9 μm (filled symbols, $P < 0.001$) and above 7 μm (open symbols, $P < 0.001$) in the right sural nerve. (B) The SNAP amplitudes in the right median nerve, left sural nerve, and right sural nerve were correlated with the mean diameters of the 10 largest fibers in the right sural nerve ($P < 0.001$). (C) Correlation between the measured sensory nerve conduction velocities (SNCV) in the right median nerve, left sural nerve, and right sural nerve and the theoretical SNCV calculated from the mean diameters of the 10 largest fibers in the right sural nerve using a conversion factor of 4.3 m/sec per μm.[23] The stippled line indicates the predicted conduction velocity. The lower SNCV in the patients (solid line; $P < 0.001$) is consistent with demyelination.

Relationship between (lyso)sulfatide levels and neuropathy

The number of myelinated sural nerve fibers ≥9 μm in diameter correlated with sulfatide concentration ($P < 0.05$) as did the log of the median and sural SNAP amplitudes ($P < 0.05$) and the median and sural SNCVs ($P < 0.05$).

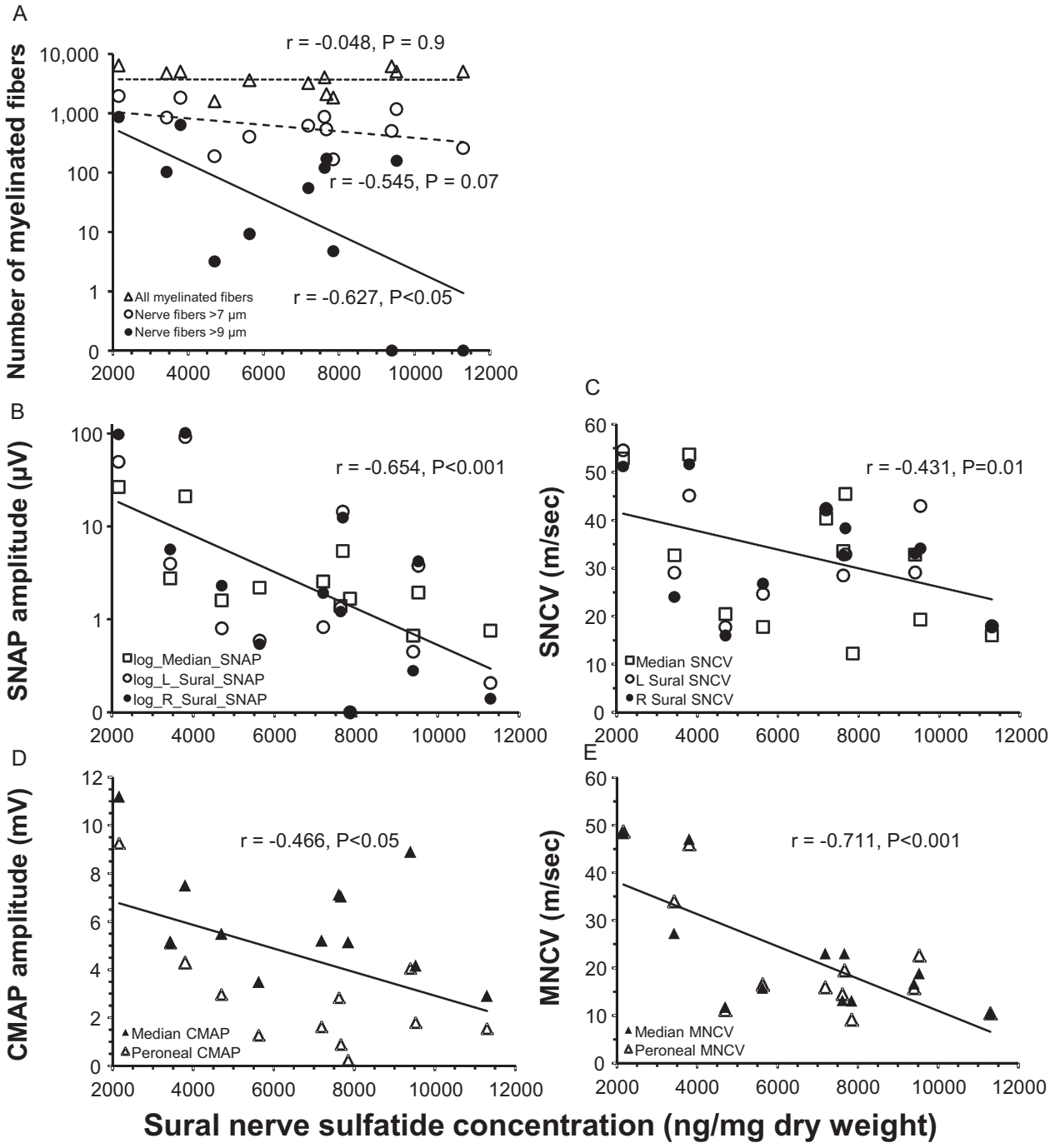

Figure 6. Relationships between sural nerve sulfatide concentration and myelinated fibers and nerve conduction studies in late infantile metachromatic leukodystrophy. (A) Number of myelinated fibers in the right sural nerve (fibers >9 μm, $P < 0.05$; fibers >7 μm, $P = 0.07$; all fibers, $P = 0.9$). (B) Pooled amplitudes of sensory nerve action potentials (SNAP) in the right median, left sural, and right sural nerves. (C) Pooled sensory nerve conduction velocities (SNCV) in the right median, left sural, and right sural nerves. (D) Pooled amplitudes of compound muscle action potentials (CMAP) in the right median and peroneal nerves. (E) Pooled motor nerve conduction velocities (MNCV) in the right median and peroneal nerves.

The MNCV and CMAP of the median and peroneal nerves also correlated with sural nerve sulfatide concentration ($P < 0.05$, Fig. 6).

The median and tibial SSEP cortical latencies and central conduction times did not correlate with sural nerve sulfatide content, whereas the median peripheral latencies

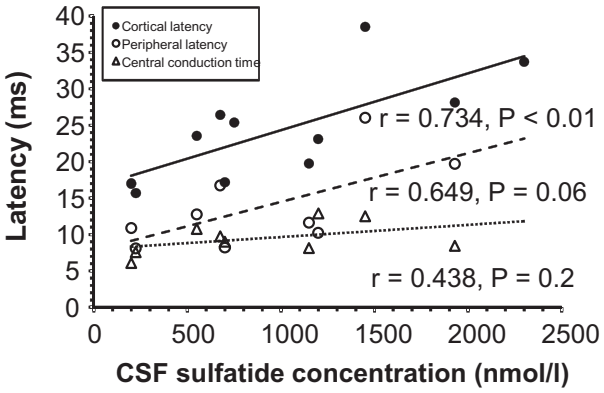

Figure 7. Relationship between the cerebrospinal fluid sulfatide concentration and median nerve somatosensory evoked potentials (SSEP). The latencies of the cortical responses correlated with the sulfatide concentration ($P < 0.01$) and the peripheral latencies trended toward significance ($P = 0.06$). The central conduction time was not correlated with the sulfatide concentration.

correlated with the sural nerve content. The median SSEP cortical ($P < 0.01$) and peripheral nerve ($P = 0.056$) latencies correlated with cerebrospinal sulfatide concentration; central conduction time, however, did not (Fig. 7). The tibial SSEP cortical latency trended toward significance ($P < 0.1$).

Discussion

The disease process in late infantile MLD is characterized by progressive neurodegeneration and early mortality. Both the PNS and the CNS are involved with devastating motor and cognitive decline leading to loss of speech and ambulation during the first years after onset of symptoms.[24] The disorder is associated with accumulation of 3-*O*-sulfogalactosylceramide (sulfatide) due to reduced activity of ASA, which is caused by mutations in the gene located on chromosome 22q13.31–qter. The mutations reported here are heterogeneous and not predictive of phenotype as previously described in the literature.[1] Studies in murine models of MLD indicate that disease pathology is due in part to the accumulation of sulfatide. Sulfatide is normally present in oligodendrocytes and Schwann cells and is necessary for the development and maintenance of myelin[25–27]; in its absence fibers show severe dysmyelination and ion-channel dysregulation.[28] Recently it has become clear that a derivative of sulfatide, lysosulfatide, is involved in cellular calcium homeostasis. When lysosulfatide is added to cells in vitro, Ca^{2+} levels increase causing activation of intracellular proteases and cellular injury.[29]

We examined the relationship between motor and sensory function and CSF and sural nerve (lyso)sulfatide levels in 13 children with late infantile MLD. There is no approved therapy for late infantile MLD, but gene and enzyme replacement therapies are now being tested in clinical trials.[30–33] In this context, it is important to have sensitive biomarkers that correlate with disease severity and are dose-responsive to therapeutic interventions.

Slowing of conduction was uniform in different nerves in the arms and legs as has been described in other studies of patients with MLD[3] and other types of hereditary demyelinating neuropathy.[34] Moreover, the amplitudes and conduction velocities of motor and sensory responses were linearly correlated supporting the generalized distribution of demyelination. In contrast, we did not find evidence of multifocal involvement as has been claimed in other studies.[35] However, the excitability of peripheral nerves was reduced as indicated by the extremely large increase in threshold, which in some cases erroneously may be interpreted as conduction block if maximal stimulation cannot be attained.

The process of demyelination and fiber loss in the PNS of patients with MLD has been well documented in the literature.[36–38] Electron micrographs show characteristic inclusion bodies and light microscopy (LM) reveals metachromatically stained sulfatide granules within the cytoplasm of Schwann cells in all nerves. In the present study, we found impaired PNS function with very low nerve conduction velocities and SNAPs associated with loss of large fibers, thin myelin sheaths (Fig. 5), and increased *g*-ratios as indicated by the correlation between the *g*-ratios and the right sural nerve SNAP log-amplitudes and SNCVs ($P < 0.05$).

The abnormalities observed in CSF and sural neve (lyso)sulfatide levels and NCS did not correlate with CNS disease burden as measured by motor function assessment (GMFM-88) and NAA levels in the centrum semiovale. Similar discordance between NCS studies and clinical examination has previously been reported in a large cohort of MLD patients[36] and in other demyelinating disorders of the PNS.[34] In our case series, this point is illustrated by two patients (1 and 12) who were still able to walk despite motor conduction velocities of 23 m/sec. Furthermore, two patients had normal peripheral nerve conduction; one was still able to walk and the other was only able to sit. LM of the sural nerves in the latter patients showed minimal demyelination, whereas electron microscopy (EM) showed inclusion bodies in Schwann cells and abnormal *g*-ratios. SSEPs were delayed suggesting central involvement. To our knowledge normal NCS and LM findings have been described in only a few cases of adult–onset MLD and EM examination of the sural nerve in one revealed demyelination.[39,40] The two children with normal NCS in our series had mildly increased sural nerve sulfatide levels raising the possibility of a distinctive genotype/phenotype correlation. However, in

the present series of patients with several different mutations, there was no discernible relationship between the (lyso)sulfatide levels, the electrophysiological findings, or the clinical presentation and the particular mutations. The EM pictures of all other patients showed pronounced demyelination and numerous inclusion bodies and masses of cell debris.[37,38]

In a recent investigation of regeneration in injured nerves, it was concluded that sulfatide plays a major role in the inhibition of axonal outgrowth.[41] This observation together with the understanding that sulfatide also has a role in oligodendrocyte differentiation and the communication between Schwann cells and axons could explain how (lyso)sulfatide content influences nerve function.[26] The correlations between standardized measures of PNS function and levels of sulfatide are intriguing since they underscore the pathophysiologic relationship between a biomarker and functional status. Our findings suggest that the main pathological abnormalities are demyelination with preserved axonal caliber; axonal loss occurs with advanced disease. Our data indicate that the extent of sulfatide and lysosulfatide accumulation within sural nerve and CSF is directly proportional to the severity of damage to peripheral nervous tissue, whereas these markers do not reflect the extent of CNS damage. Similar findings have been reported in an ASA-deficient mouse model where accumulation of sulfatide increased with age and correlated with histological damage to peripheral nerves.[42] Sulfatide and lysosulfatide levels provide a measure of the extent of local tissue injury. For the patients reported here the average sural nerve sulfatide concentration is estimated to be ~35,000-fold greater on a molar basis than the corresponding CSF values. We suggest that the CSF sulfatide level provides a marker reflective of disease burden in the intraspinal nerve roots and PNS; it does not mirror the extent of central white matter injury as stated previously.

Acknowledgment

The study was sponsored by Shire. Support was provided by the Danish Medical Research Council, the Lundbeck Foundation, and the Novo Nordisk Foundation (M. M., C. K.). The authors are deeply appreciative of the many contributions made to this work by Jack Griffin before his untimely death on 16 April 2011.

Author Contribution

Christine i. Dali: Study design and coordinator, clinical-MRI-electrophysiological study, data analysis and interpretation, manuscript development; christine.dali@regionh.dk. Norman Barton: Study design, data analysis and interpretation; manuscript development; nbarton@shire.com. Mohamed Farah: Ultrastructural analysis of MLD nerves; mfarah2@jhu.edu. Mihai Moldovan: development of software for nerve morphometry and morphometry of nerves from MLD patients; moldovan@sund.ku.dk. Jan-Eric Månsson: Analysis of sulfatide in spinal fluid; jan-eric.mansson@vgregion.se. Nitin Nair: Data analysis and statistics; manuscript development; nnair_25@yahoo.com. Morten Dunø: molecular gene analysis and interpretation; morten.dunoe@regionh.dk. Lotte Risom: molecular gene analysis and interpretation; lotte.risom@regionh.dk. Hongmei Cao: LC/MS/MS analysis of sural nerve sulfatide and lysosulfatide; hcao@shire.com. Luying Pan: Analysis of ASA cross-reactive immunological material (CRIM) in fibroblasts; lpan@shire.com. Marcia Sellos-Moura: CRIM and LC/MS/MS data analysis and interpretation; msellos@shire.com. Andrea Corse: Morphological analysis of control nerves from Johns Hopkins; acorse@jhmi.edu. Christian Krarup: Study design, electrophysiological studies, data analysis and interpretation, manuscript development; christian.krarup@regionh.dk.

Conflict of Interest

Dr. í Dali has been salaried by Shire, and Dr. Krarup has received consulting honorarium from Shire. Drs. Barton, Cao, Pan and Sellos-Moura are employees of Shire. Dr. Nair was an employee of Shire at the time of performing the work in the paper.

References

1. Gieselmann V. Metachromatic leukodystrophy: genetics, pathogenesis and therapeutic options. Acta Paediatr Suppl 2008;97:15–21.
2. Biffi A, Cesani M, Fumagalli F, et al. Metachromatic leukodystrophy – mutation analysis provides further evidence of genotype-phenotype correlation. Clin Genet 2008;74:349–357.
3. Miller RG, Gutmann L, Lewis RA, Sumner AJ. Acquired versus familial demyelinative neuropathies in children. Muscle Nerve 1985;8:205–210.
4. Zafeiriou DI, Kontopoulos EE, Michelakakis HM, et al. Neurophysiology and MRI in late-infantile metachromatic leukodystrophy. Pediatr Neurol 1999;21:843–846.
5. Toda K, Kobayashi T, Goto I, et al. Lysosulfatide (sulfogalactosylsphingosine) accumulation in tissues from patients with metachromatic leukodystrophy. J Neurochem 1990;55:1585–1591.
6. Rosenbaum PL, Palisano RJ, Bartlett DJ, et al. Development of the Gross Motor Function Classification System for cerebral palsy. Dev Med Child Neurol 2008;50:249–253.

7. Russell DJ, Avery LM, Rosenbaum PL, et al. Improved scaling of the gross motor function measure for children with cerebral palsy: evidence of reliability and validity. Phys Ther 2000;80:873–885.
8. Miller SA, Dykes DD, Polesky HF. A simple salting out procedure for extracting DNA from human nucleated cells. Nucleic Acids Res 1988;16:1215.
9. Livak KJ, Schmittgen TD. Analysis of relative gene expression data using real-time quantitative PCR and the 2 (-Delta Delta C(T)) Method. Methods 2001;25:402–408.
10. Davidsson P, Fredman P, Mansson JE, Svennerholm L. Determination of gangliosides and sulfatide in human cerebrospinal fluid with a microimmunoaffinity technique. Clin Chim Acta 1991;197:105–115.
11. Kristjansdottir R, Uvebrant P, Lekman A, Mansson JE. Cerebrospinal fluid markers in children with cerebral white matter abnormalities. Neuropediatrics 2001;32:176–182.
12. i Dali C, Hanson LG, Barton NW, et al. Brain *N*-acetylaspartate levels correlate with motor function in metachromatic leukodystrophy. Neurology 2010;75:1896–1903.
13. Wagner AL, Buchthal F. Motor and sensory conduction in infancy and childhood: reappraisal. Dev Med Child Neurol 1972;14:189–216.
14. Garcia A, Calleja J, Antolin FM, Berciano J. Peripheral motor and sensory nerve conduction studies in normal infants and children. Clin Neurophysiol 2000;111:513–520.
15. Fagan ER, Taylor MJ, Logan WJ. Somatosensory evoked potentials: Part II. A review of the clinical applications in pediatric neurology. Pediatr Neurol 1987;3:249–255.
16. Taylor MJ, Fagan ER. SEPs to median nerve stimulation: normative data for paediatrics. Electroencephalogr Clin Neurophysiol 1988;71:323–330.
17. Gilmore R. The use of somatosensory evoked potentials in infants and children. J Child Neurol 1989;4:3–19.
18. Krarup C. Compound sensory action potential in normal and pathological human nerves. Muscle Nerve 2004;29:465–483.
19. Polten A, Fluharty AL, Fluharty CB, et al. Molecular basis of different forms of metachromatic leukodystrophy. N Engl J Med 1991;324:18–22.
20. Parano E, Uncini A, De Vivo DC, Lovelace RE. Electrophysiologic correlates of peripheral nervous system maturation in infancy and childhood. J Child Neurol 1993;8:336–338.
21. Jacobs JM, Love S. Qualitative and quantitative morphology of human sural nerve at different ages. Brain 1985;108:897–924.
22. Behse F. Morphometric studies on the human sural nerve. Acta Neurol Scand 1990;82:5–38.
23. Behse F, Buchthal F. Sensory action potentials and biopsy of the sural nerve in neuropathy. Brain 1978;101:473–493.
24. Kehrer C, Blumenstock G, Raabe C, Krageloh-Mann I. Development and reliability of a classification system for gross motor function in children with metachromatic leucodystrophy. Dev Med Child Neurol 2011;53:156–160.
25. Baron W, Ozgen H, Klunder B, et al. The major myelin-resident protein PLP is transported to myelin membranes via a transcytotic mechanism: involvement of sulfatide. Mol Cell Biol 2015;35:288–302.
26. Marcus J, Honigbaum S, Shroff S, et al. Sulfatide is essential for the maintenance of CNS myelin and axon structure. Glia 2006;53:372–381.
27. Eckhardt M. The role and metabolism of sulfatide in the nervous system. Mol Neurobiol 2008;37:93–103.
28. Hayashi A, Kaneko N, Tomihira C, Baba H. Sulfatide decrease in myelin influences formation of the paranodal axo-glial junction and conduction velocity in the sciatic nerve. Glia 2013;61:466–474.
29. Hans M, Pusch A, Dai L, et al. Lysosulfatide regulates the motility of a neural precursor cell line via calcium-mediated process collapse. Neurochem Res 2009;34:508–517.
30. Shapiro EG, Lockman LA, Balthazor M, Krivit W. Neuropsychological outcomes of several storage diseases with and without bone marrow transplantation. J Inherit Metab Dis 1995;18:413–429.
31. Sevin C, Aubourg P, Cartier N. Enzyme, cell and gene-based therapies for metachromatic leukodystrophy. J Inherit Metab Dis 2007;30:175–183.
32. Biffi A, Capotondo A, Fasano S, et al. Gene therapy of metachromatic leukodystrophy reverses neurological damage and deficits in mice. J Clin Invest 2006;116:3070–3082.
33. Matzner U, Herbst E, Hedayati KK, et al. Enzyme replacement improves nervous system pathology and function in a mouse model for metachromatic leukodystrophy. Hum Mol Genet 2005;14:1139–1152.
34. Garcia A, Combarros O, Calleja J, Berciano J. Charcot-Marie-Tooth disease type 1A with 17p duplication in infancy and early childhood: a longitudinal clinical and electrophysiologic study. Neurology 1998;50:1061–1067.
35. Cameron CL, Kang PB, Burns TM, et al. Multifocal slowing of nerve conduction in metachromatic leukodystrophy. Muscle Nerve 2004;29:531–536.
36. Bindu PS, Mahadevan A, Taly AB, et al. Peripheral neuropathy in metachromatic leucodystrophy. A study of 40 cases from south India. J Neurol Neurosurg Psychiatry 2005;76:1698–1701.
37. Bardosi A, Friede RL, Ropte S, Goebel HH. A morphometric study on sural nerves in metachromatic leucodystrophy. Brain 1987;110:683–694.
38. Martin JJ, Ceuterick C, Mercelis R, Joris C. Pathology of peripheral nerves in metachromatic leucodystrophy. A

comparative study of ten cases. J Neurol Sci 1982;53:95–112.
39. Marcao AM, Wiest R, Schindler K, et al. Adult onset metachromatic leukodystrophy without electroclinical peripheral nervous system involvement: a new mutation in the ARSA gene. Arch Neurol 2005;62:309–313.
40. Gallo S, Randi D, Bertelli M, et al. Late onset MLD with normal nerve conduction associated with two novel missense mutations in the ASA gene. J Neurol Neurosurg Psychiatry 2004;75:655–657.
41. Winzeler AM, Mandemakers WJ, Sun MZ, et al. The lipid sulfatide is a novel myelin-associated inhibitor of CNS axon outgrowth. J Neurosci 2011;31:6481–6492.
42. Matthes F, Stroobants S, Gerlach D, et al. Efficacy of enzyme replacement therapy in an aggravated mouse model of metachromatic leukodystrophy declines with age. Hum Mol Genet 2012;21:2599–2609.

